Article

Effects of Process Design on Recycle Dynamics and Its Implication to Control Structure Selection

Yu-Chang Cheng, and Cheng-Ching Yu

Ind. Eng. Chem. Res., **2003**, 42 (19), 4348-4365 • DOI: 10.1021/ie020799i

Effects of Process Design on Recycle Dynamics and Its Implication to Control Structure Selection

Yu-Chang Cheng[†] and Cheng-Ching Yu*[,‡]

Department of Chemical Engineering, National Taiwan University of Science and Technology, Taipei 106-07, Taiwan, and Department of Chemical Engineering, National Taiwan University, Taipei 106-17, Taiwan

In this paper we explore the dynamics of simple recycle plants under different process designs using different control structures. A simple reactor/separator process with a first-order irreversible reaction is studied. From transfer-function-based linear analysis, we are able to derive recycle dynamics for the entire range of conversion, the most important design parameter for the simple recycle plant. Under the conventional control structure (constant reactor holdup practice), the results indicate that we have exactly the *same* input/output (fresh feed to the production rate dynamics), irrespective of reactor conversions. The linear analysis is validated using rigorous nonlinear simulation via a step-by-step relaxation on model assumptions. It turns out that reactor level control plays the most important role in the input/output dynamics. The analysis is extended to the balanced control structure, a control strategy with variable reactor holdup. The results show that, different from the previous case, a larger conversion implies slower input/output dynamics. Ongoing analyses indicate that the inherent dynamics of the recycle plant depend on the process design as well as the fundamental control principle. Finally, implications to control structure design are also given for different levels of reactor conversions.

1. Introduction

Because of stringent environmental regulations and economic considerations, today's chemical plants tend to be highly integrated and interconnected. The steady-state and dynamic behaviors of these interconnected units differ significantly from individual counterparts.[5,14,15,19,23] A typical plant configuration is the reactor/separator processes with material recycles where unreacted reactants are recycled back to the reactor. Dynamics and control of processes with recycle streams received less attention until recent years.

Early research includes the pioneering work of Gilliland et al.,[7] who explained the dynamics of a reactor/separator system. They point out that the effect of the recycle stream increases the time constants of the process. Verykios and Luyben[27] studied a slightly more complex process with simplified column dynamics, and they showed that these recycle systems can exhibit underdamped behavior. Denn and Lavie[5] also showed that the response time of recycle systems can be substantially longer than the response time of individual units. Recently, Luyben[14,15,18] investigated the effects of recycle loops on process dynamics and their implications to plantwide control. Taiwo[26] proposed the concept of recycle compensation, Scali and Ferrari[23] derived a recycle compensator to reinstall inherent process dynamics (dynamics without recycle), and similar approaches were extended by Lakshminarayanan and Takada[12] and Kwok et al.[11]

It is well-known that, topologically, material recycle in an interconnected process is equivalent to a positive feedback system with a loop gain of less than unity. In a typical positive feedback configuration, if we increase the loop gain, two features become apparent: (1) it slows down the process dynamics and (2) it increases the steady-state gain in the direct path.[3,5,14,19,23] However, in a reactor/separator process, we have a very different scenario. A smaller recycle flow translates into a larger reactor conversion and, thus, slower reactor dynamics. How do these competing effects affect the dynamics of the positive feedback system and what are the implications of these effects on control structure design?

The issue of nonlinear analysis (bifurcation and the like) for recycle plants has been an active area of research.[1,10,22] The nonlinear analysis provides a *global* view on system stability and sensitivity over the entire design range (e.g., Bildea et al.[1]). The bifurcation diagrams permit one to determine the stability of the designed process and to evaluate the sensitivity of certain design or operating parameters. On the contrary, the linear analysis zooms into a specific design condition and gives a quantitative description of linear dynamics (e.g., transfer function between variables), a *local* method. However, if the model parameters are expressed in terms of system (e.g., rate constant) and design (e.g., conversion) parameters, the local model can be used to analyze dynamics over the entire design range, a local model analyzing global behavior. This is exactly the objective of this paper.

This paper aims to explore the dynamics of a simple reactor/separator process under different process designs, and the implications to control structure selection will also be given. In section 2, simple process transfer functions are derived from material balances and recycle dynamics are explored. This facilitates the assessment of recycle dynamics at the design stage. In section 3, assumptions such as a linear reactor model, perfect level control, and perfect separation are relaxed and the dominant variable on input/output dynamics is also explored. The linear analysis is extended to a different control structure and similarity and difference are

* To whom correspondence should be addressed. Tel.: +886-2-3365-1759. Fax: +886-2-2362-3040. E-mail: ccyu@ntu.edu.tw.
[†] National Taiwan University of Science and Technology.
[‡] National Taiwan University.

10.1021/ie020799i CCC: $25.00
Published on Web 08/19/2003

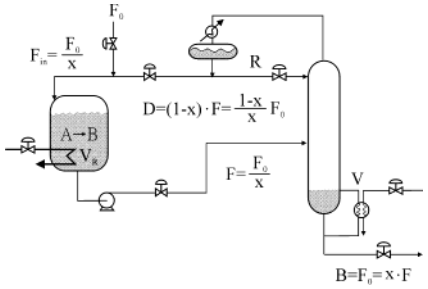

Figure 1. Reactor/separator recycle process.

contrasted in section 4. Implications to control structure design are given in section 5 followed by the conclusion in section 6.

2. Linear Analysis

2.1. Process and Design Alternatives. A simple reactor/separator process is used to illustrate the effects of design and control structure selection.[21,28,29] The process consists of a reactor and a distillation column in an interconnected structure as shown in Figure 1. The reaction is irreversible, A → B, with first-order kinetics.

$$R = V_R k z_A \tag{1}$$

Here R is the reaction rate (mol/h), k is the rate constant (h^{-1}), V_R is the reactor holdup (mol), and z_A is the mole fraction of the reactant A. The effluent of the reactor (F in mol/h) is fed into a distillation column. The product B is removed from the bottom of the column. The purified reactant is recycled back to the reactor via the distillate flow. Note that, unless otherwise mentioned, all compositions and holdups are expressed in terms of mole fraction and moles. Figure 1 describes the flow rates in the recycle process under different reactor conversion (x).

$$x = \frac{z_{A0} - z_A}{z_{A0}} \tag{2}$$

Note that these flow rates are obtained from material balances with the assumptions of perfect separation and pure reactant (i.e., $z_{A0} = 1$).

The conversion (x) is the dominant design variable for the simple recycle process. We can design the reactor with a small conversion (x) coupled with a distillation column large in diameter (for increased vapor/liquid flows), or one can make the reactor conversion large, connected to a moderately sized (in diameter) column. Note that the Fenske equation shows that the tray numbers are the same as long as the separation specifications remain the same. Steady-state economics of these alternatives are important in process design,[15] but we are interested in recycle dynamics at the design stage.

Before we get into the model derivation, three plant-wide control principles are contrasted. In addition to necessary level and composition loops in plantwide control, one of the most important decisions to make is to set the throughput manipulator.[4,17] Thus, we have to decide which variable should handle the production rate changes. As can be seen from eq 1, three likely candidates are reactor composition (changing z_A via recycle flow[4,14,15]), reactor holdup (changing V_R[28,29]), and reactor temperature (changing k via reactor temperature). In a general way, these three control principles are termed as control structure 1 (CS1), control structure 2 (CS2), and control structure 3 (CS3), respectively. The first case is studied here, and we will extend the other two cases in a later section.

2.2. Linear Model. CS1 is often referred to as the conventional structure, where the recycle flow is changed to accommodate production rate variation. This implies a constant reactor holdup.

2.2.1. Reactor. In a series of papers,[6,16,18] Luyben and co-workers investigated tradeoffs between design and control of chemical reactor systems. A similar approach is taken here with different definitions on state variables. Consider the reactor in Figure 1 where F_{in} is the reactor feed, F is the reactor effluent, and V_R is the reactor holdup. The component material balance for A is

$$\frac{dV_R z_A}{dt} = F_{in} z_{A0} - F z_A - k V_R z_A \tag{3}$$

Generally, reactant concentrations, z_A and z_B, are state variables. However, in the analysis of the recycle process, it is more convenient to use the total outflow of components A and B, F_A and F_B, as state variables.

$$F_A = F z_A \qquad \text{and} \qquad F_B = F z_B \tag{4}$$

Assuming perfect level control (V_R = constant and $F_{in} = F$) and a pure reactant ($z_{A0} = 1$) and substituting eq 4 into the balance equation (eq 3), we have

$$\frac{dF_A}{dt} - \frac{F_A}{F}\frac{dF}{dt} = \frac{F^2}{V_R} - \frac{F F_A}{V_R} - k F_A \tag{5}$$

Linearizing eq 5 and taking Laplace transformation, one obtains

$$\frac{F_A(s)}{F(s)} = \frac{\dfrac{\bar{F}_A}{\bar{F}}s + \left(\dfrac{2\bar{F}}{\bar{V}_R} - \dfrac{\bar{F}_A}{\bar{V}_R}\right)}{s + \left(\dfrac{\bar{F}}{\bar{V}_R} + k\right)} \tag{6}$$

where the overbar stands for a nominal steady-state value. Note that, to obtain a correct linearization result, the time derivative of F in the left-hand side of eq 5 is treated as an independent variable. Because we would like to characterize the reactor size using the conversion, assuming pure reactant A and from steady-state material balances, we have

$$\tau_R = \frac{\bar{V}_R}{\bar{F}} = \frac{x}{k(1-x)} \tag{7}$$

where τ_R is the reactor residence time. When eqs 4 and 7 are substituted into eq 6, the relationship between the total outflow of A and the total reactor feed becomes

$$\frac{F_A(s)}{F_{in}(s)} = \frac{\dfrac{x(1-x)}{k}s + (1-x^2)}{\dfrac{x}{k}s + 1} \tag{8}$$

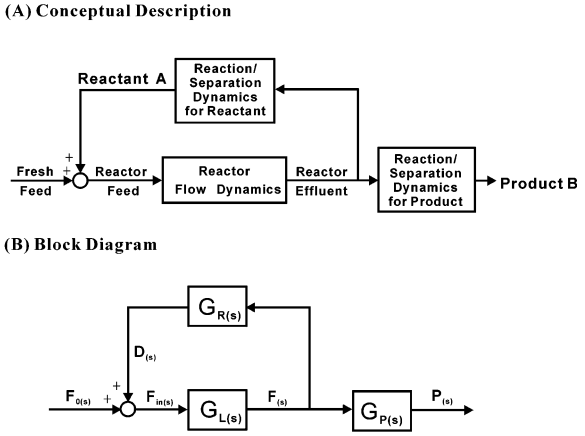

Figure 2. Conceptual description (A) and block diagram (B) for the reactor/separator process.

A similar result can be obtained for component B.

$$\frac{F_B(s)}{F_{in}(s)} = \frac{\frac{x^2}{k}s + x^2}{\frac{x}{k}s + 1} \tag{9}$$

Note that the steady-state gains in eqs 8 and 9 are different from those of the composition-based expression. Equations 8 and 9 clearly indicate that an increased conversion, indeed, slows down the reactor dynamics as seen in the movement of the pole location ($p = -k/x$ where p denotes pole). It reveals that, at low conversion, the pole is located at the far left of the s plane and, as the conversion increases, the pole approaches $-k$. Moreover, the low limit of the reactor dynamics is characterized by the fundamental chemistry, the reaction rate constant ($p = -k$).

2.2.2. Recycle Plant. With appropriate parametrization, we can incorporate the reactor models into the recycle process. The recycle process consists of a reactor and a separator (Figure 1). Assuming *perfect separation with no separator dynamics*, all of the unreacted reactant A (F_A) is recycled back to the reactor and the product B (F_B) is taken out from the separator instantaneously. Therefore, a block diagram can be constructed to describe the recycle process. Note that this work differs from the previous modeling in that the outflows of different components (F_A and F_B) are used as state variables and the interaction between flow (F) and composition (z_A and z_B) can be avoided.

Figure 2A describes the basic idea where the reaction/separation dynamics is lumped together for the recycle part (G_R for reactant A) and for the product part (G_P for product B) and the reactor flow dynamics (G_L) is placed between the reactor influent and effluent. Because perfect level control is assumed, we have

$$G_L(s) = 1 \tag{10}$$

With the perfect separation assumption, the recycle flow and product flow dynamics are

$$G_R = F_A(s)/F(s) \tag{11}$$

$$G_P = F_B(s)/F(s) \tag{12}$$

Notice that if separator dynamics is not negligible and separation is far from perfect, additional lags and

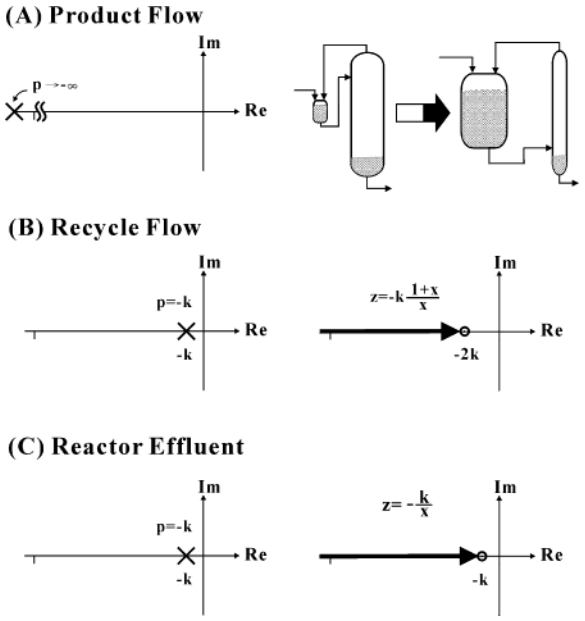

Figure 3. Root locus with varying conversion for the reactor/separator process with CS1 for (A) product flow dynamics (× indicating a fixed pole), (B) recycle flow dynamics (× indicating a fixed pole and ○ denoting converging zero location), and (C) reactor flow dynamics (× indicating a fixed pole and ○ denoting converging zero location).

separation gains (fractional recovery) can be included in G_R and G_P. Substituting the analytical expressions (eqs 8 and 9) into the positive feedback structure (Figure 2B), we are able to analyze the dynamics for the recycle process with alternative process designs.

$$\frac{P(s)}{F_0(s)} = \frac{G_L G_P}{1 - G_L G_R} = 1 \tag{13}$$

$$\frac{D(s)}{F_0(s)} = \frac{G_L G_R}{1 - G_L G_R} = \frac{\frac{1-x}{kx}s + \frac{1-x^2}{x^2}}{\frac{1}{k}s + 1} \tag{14}$$

$$\frac{F(s)}{F_0(s)} = \frac{G_L}{1 - G_L G_R} = \frac{\frac{1}{kx}s + \frac{1}{x^2}}{\frac{1}{k}s + 1} \tag{15}$$

where F_0 denotes the fresh feed, P stands for the production rate, and D is the recycle flow. Several observations can be made from these immediately.

1. Regardless of the design alternatives (different conversions), perfect production changes can always be achieved as shown in Figure 3. Equation 13 defines the *input/output* dynamics.

2. For different conversions (x) in design, the poles of *internal* flow dynamics [$D(s)/F_0(s)$ and $F(s)/F_0(s)$] are invariant and they are located at $p = -k$ as shown in parts B and C of Figure 3.

3. The zeros of *internal* flow dynamics [$D(s)/F_0(s)$ and $F(s)/F_0(s)$] start from far left at low conversion ($x \to 0$) and converge to $-2k$ and $-k$ at high conversion ($x \to 1$) for recycle and reactor feed flow dynamics, respectively (parts B and C of Figure 3).

4. The steady-state sensitivity of the recycle flow (D) to the fresh feed flow (F_0) varies from infinity to 0 as the conversion (x) changes from 0 to 1 as indicated by

Table 1. Parameter Values and Steady-State Conditions for Reactor/Separator Systems

	$x = 0.2$	$x = 0.5$	$x = 0.9$
CSTR			
fresh feed flow rate (F_0) (lb·mol/h)	460	460	460
fresh feed composition (z_0)	0.9	0.9	0.9
fresh feed temperature (T_0) (°R)	530	530	530
recycle flow rate (D) (lb·mol/h)	2421	500.4	48.44
recycle stream composition (x_D)	0.95	0.95	0.95
recycle stream temperature (T_D) (°R)	587.2	587.2	587.2
reactor temperature (T) (°R)	616.4	616.4	616.4
reactor holdup (V_R) (lb mol)	1501	2401	12005
activation energy (E) (Btu/lb·mol)	30842	30842	30842
Distillation			
column feed flow rate (F) (lb·mol/h)	2881	960.4	508.4
column feed composition (z_A)	0.8	0.5	0.1
reflux flow rate (R) (lb·mol/h)	1861	1100	599
vapor boilup (V) (lb·mol/h)	4282	1600	648
no. of trays (N_T)	20	20	20
feed tray (N_F)	15	12	8
liquid hydraulic time constant (β) (s)	4	4	4
bottom holdup (M_B) (lb·mol)	275	275	275
reflux drum holdup (M_D) (lb·mol)	185	185	185
tray holdup (M_n) (lb·mol/tray)	23.5	23.5	23.5
bottom composition (x_B)	0.0105	0.0105	0.0105
bottom flow rate (B) (lb·mol/h)	460	460	460

the steady-state gain, eq 14. In terms of absolute flow rates, the ratio is $D/F_0 = (1 - x^2)/x^2$ and, expressed in percent deviation, the ratio becomes $(D/\bar{D})/(F_0/\bar{F}_0) = (1 + x)/x$.

It should be emphasized here that these observations are obtained under the assumptions of perfect level control and perfect separation. Observation 1 confirms the remarks made by Luyben:[15] *All of these competing effects result in a process in which the dynamics of various alternative designs are quite similar*. However, it is derived analytically here, and it is the most important result of this work because it points out that all different designs result in exactly the same input/output dynamics as long as they are assembled into the recycle structure and, subsequently, perfect production control can be achieved. The reason is that the fast reactor dynamics (with small conversion) compensates the slow dynamics that comes from large recycle (large recycle gain, e.g., eq 14). However, the internal dynamics is different; the zero dynamics varies with conversion (x) with a fixed pole location ($p = -k$), as can be seen from eqs 14 and 15. Observation 4 confirms the sensitivity problem of recycle plants at low conversion, termed by Luyben[17] as the "snowball effect". For example, for a recycle process with a conversion of 0.1 ($x = 0.1$), the recycle flow will increase 110% [$(1 + 0.1)/0.1 = 11$] in order to accommodate a 10% step increase in the fresh feed flow.

2.3. Dynamic Responses. To illustrate recycle dynamics, three design alternatives for the simple recycle process (Table 1) are studied. Because of the perfect separation assumption, parameter values are modified slightly. They belong to low conversion ($x = 0.2$), moderate conversion ($x = 0.5$), and high conversion ($x = 0.9$). The dashed lines in Figure 4 show the responses of the linear model. As expected, perfect production rate tracking can be obtained for all three designs, while the internal dynamics (recycle flow D and reactor feed $F_{in} = F$) follows similar dynamics with a time constant of

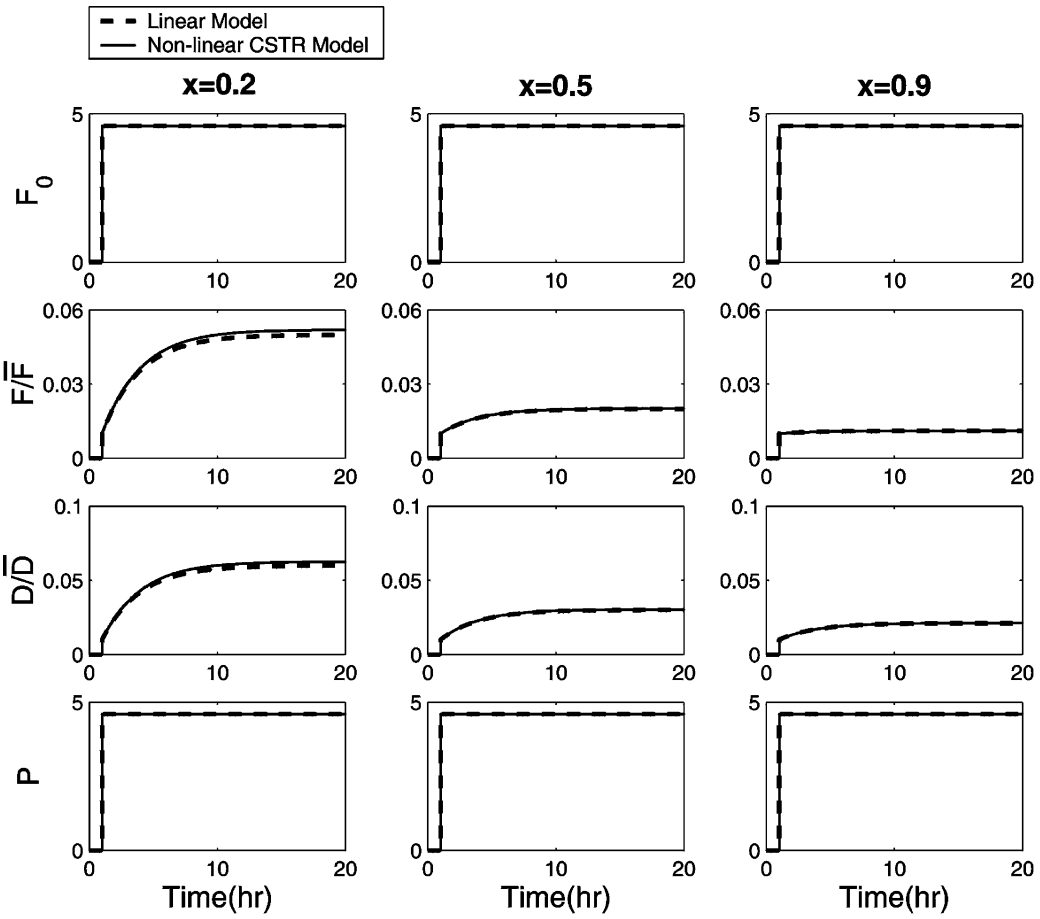

Figure 4. Reactor/separator dynamics for step change in feed flow with CS1 for different steady-state designs using a linear model (dashed lines) and a nonlinear CSTR model + perfect separator (solid lines).

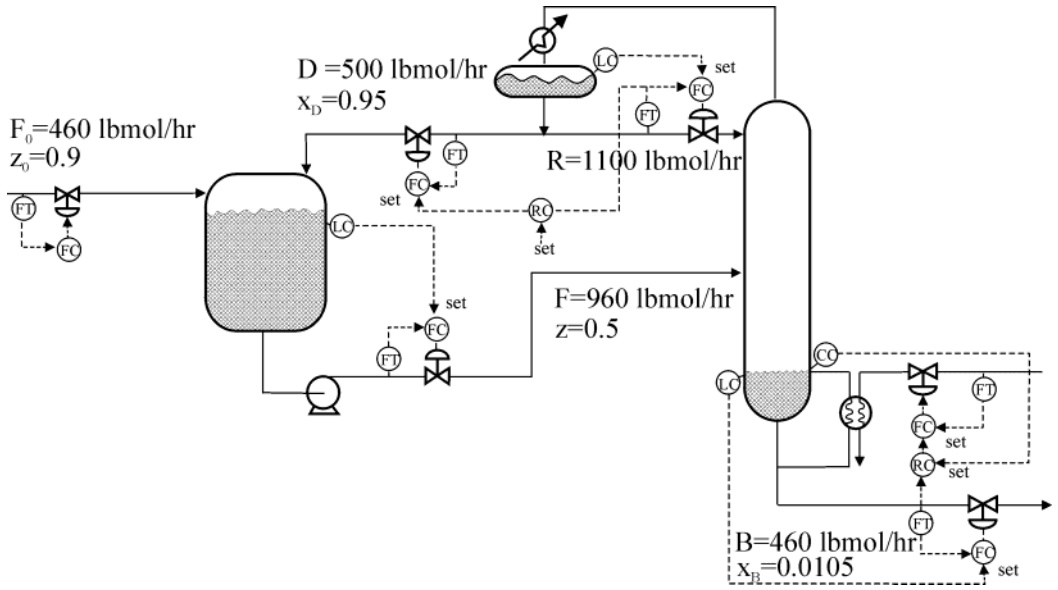

Figure 5. Control structure for the reactor/separator process (PI level controller for CS1 and P-only level controller for CS2).

$1/k$ ($p = -k$). Because the zero is approaching the pole location at high conversion for the reactor feed flow dynamics, a near pole zero cancellation is observed for the case of $x = 0.9$. As for the recycle flow sensitivity, for a 10% step increase in the production rate, the recycle flows increase 60%, 30%, and 21% ($x = 0.2$, 0.5, and 0.9).

3. Validation and Dominant Variables on Recycle Dynamics

The simulation results presented in the previous section are obtained with the following assumptions: (1) linear reactor model, (2) perfect separation with no separator dynamics, (3) perfect reactor temperature control, and (4) perfect reactor level control (for the case with constant reactor holdup). These assumptions will be lifted gradually in the following sections.

3.1. Relaxation on Modeling Assumptions. 3.1.1. Nonlinear Reactor Model. A nonlinear isothermal continuous stirred tank reactor (CSTR) model (eq 3) is placed in the recycle structure (Figure 2), and the perfect reactor level control is still assumed for this case of fixed reactor holdup. Note that, using F_A and F_B as state variables and F as the disturbance variable, we have a bilinear type of equation for the reactor, as can be seen from eq 5. This facilitates the description for processes with recycle (the recycle branch is clearly defined), but the reactor model becomes nonlinear. This means that we model the recycle process as a nonlinear CSTR with a perfect separator with no recycle dynamics. Results indicate that, for a 1% step increase in the feed flow, we have responses very similar to those obtained from a linearized model (solid lines in Figure 4). The difference is more evident at low conversions, as can be seen in Figure 4. Nonetheless, a very good approximation can be achieved using the linearized model.

3.1.2. Rigorous Distillation. Instead of assuming perfect separation, a rigorous binary distillation column is employed at this stage. The model of the distillation is similar to that in the book of Luyben[13] where $2(N_T + 2)$ ordinary differential equations were used to describe column dynamics and N_T denotes the total number of trays. A linear tray hydraulic of 4 s is assumed. The light reactant, A, is recycled back to the reactor, and the heavy product, B, is withdrawn from the bottom. The relative volatility is 2, and the product specification for the bottom is $x_B = 0.0105$, mole fraction of the light component.[28,29] Parameter values for three alternative designs are given in Table 1. Perfect reactor level control is assumed for the time being. Figure 5 shows the process flowsheet for the recycle process with $x = 0.5$. Because perfect level controls are assumed, we are left with one composition loop, controlling x_B with the boilup ratio. Relay feedback autotuning with a modified Ziegler−Nichols tuning[25] is employed to find the controller gain (K_c) and reset time (τ_I) for the proportional−integral (PI) composition controller.

Simulation results, Figure 6, clearly show that an instantaneous production change (P) can be achieved for these nonlinear recycle processes, where P is the total production of the product B, i.e., $P = (1 - x_B)B = F_B$. Comparisons between a nonlinear column (solid lines) and perfect separation (dashed lines) are also made in Figure 6. Results reveal that the linear recycle models provide a very good description of the true process, especially for moderate to large conversions (e.g., $x = 0.5$ and 0.9). Also notice that because perfect separation is assumed for the linear model, the recycle flow (D) and reactor effluent (F) are different in these two cases, but the dynamics is quite similar for both flows in these two cases.

3.2. Effect of Reactor Temperature Control. The interaction between the size and stability of the reactor is a practically important subject especially for reactor temperature control. Luyben and co-workers have studied this subject with respect to scale-up,[6] reactor configurations,[16] and autorefrigerated reactors.[18] The source of the problem is that, for a given aspect ratio, the reactor surface area (heat removal capacity) is related directly to the square of the reactor diameter while the reactor volume (heat generation) is related to the third power of the reactor diameter and, therefore, scaling up of the reactor size gives a relative reduction in the heat transfer capacity per unit volume. However, the reactor sizing problem for a recycle plant differs from the scale-up problem in that the conversion is varying. The appendix shows that, for a recycle plant, at low conver-

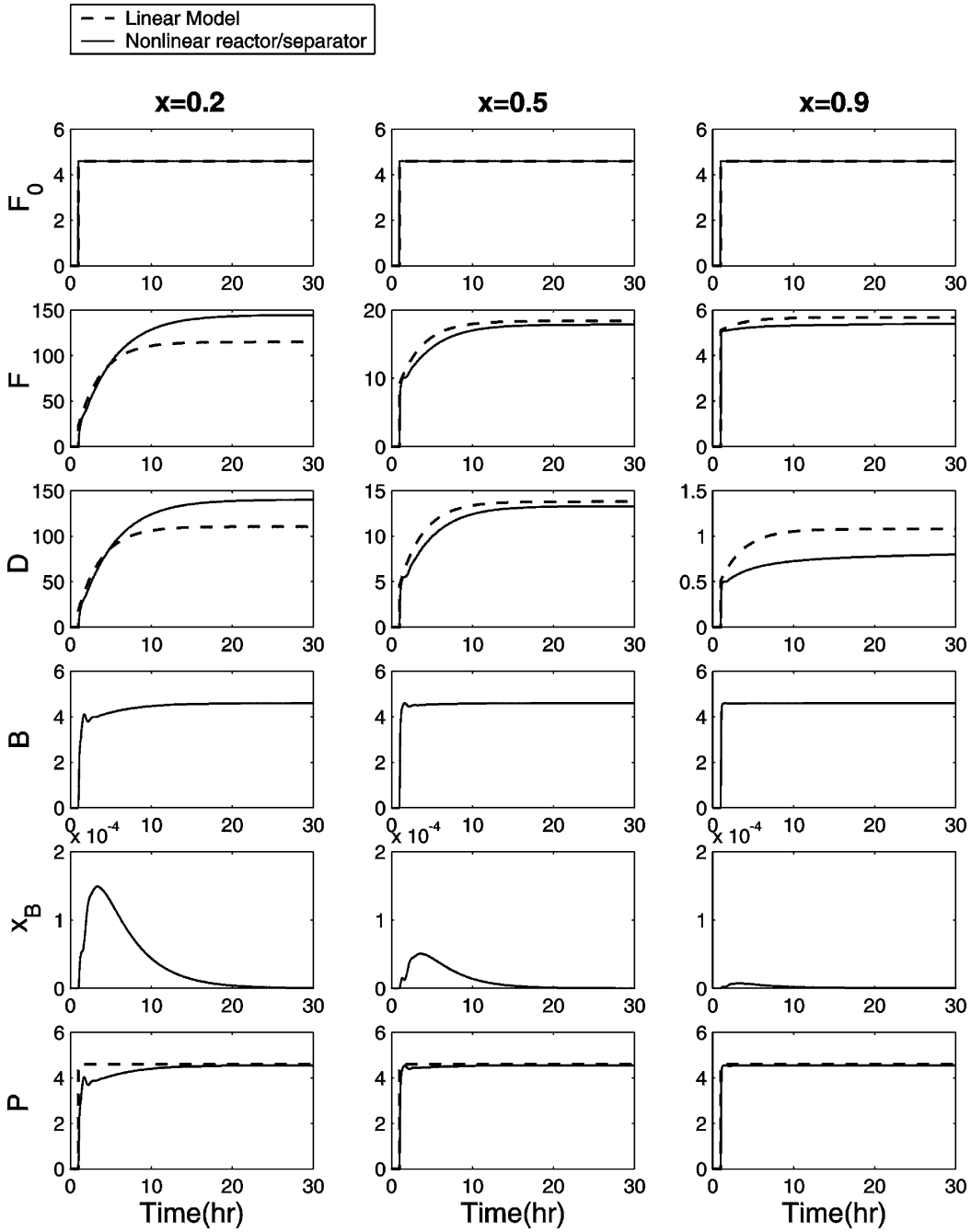

Figure 6. Reactor/separator dynamics for step change in feed flow with CS1 for different steady-state designs using a linear model (dashed lines) and a rigorous reactor/separator model + perfect reactor level control (solid lines).

sion the reactor is less controllable and the controllability improved toward high conversion. The next question then becomes, how will this affect the control of a recycle plant?

Simulation results in Figure 7 show that, indeed, better reactor temperature control can be obtained at higher conversion (see the second row of Figure 7). However, again, almost perfect production rate changes (P) can be achieved for all three conversions. Figure 5 also compares perfect (dashed lines) reactor temperature control to the nonperfect (solid lines) reactor temperature control case. Results reveal that, except for the temperature dynamics, the rest of the dynamic responses are almost identical. At least for these open-loop stable reactors, reactor temperature dynamics has little impact on the overall process dynamics. As a result, the reactor temperature control will not be addressed further in this work. Nonetheless, it is interesting to notice the controllability trend for the reactor in a recycle plant because it is just the opposite to that of reactor scaling up. In other words, in a recycle plant, a larger reactor is easier to control.

3.3. Effect of Reactor Level Control. Finally, the assumption of perfect reactor level control is relaxed. Consider the reactor level control in Figure 5 with a PI controller. The closed-loop transfer function between F_{in} and F is simply

$$G_L(s) = \frac{F}{F_{in}} = \frac{\tau_1 s + 1}{\frac{\tau_1}{K_C} s^2 + \tau_1 s + 1} \tag{16}$$

This is a second-order system, and we would like to

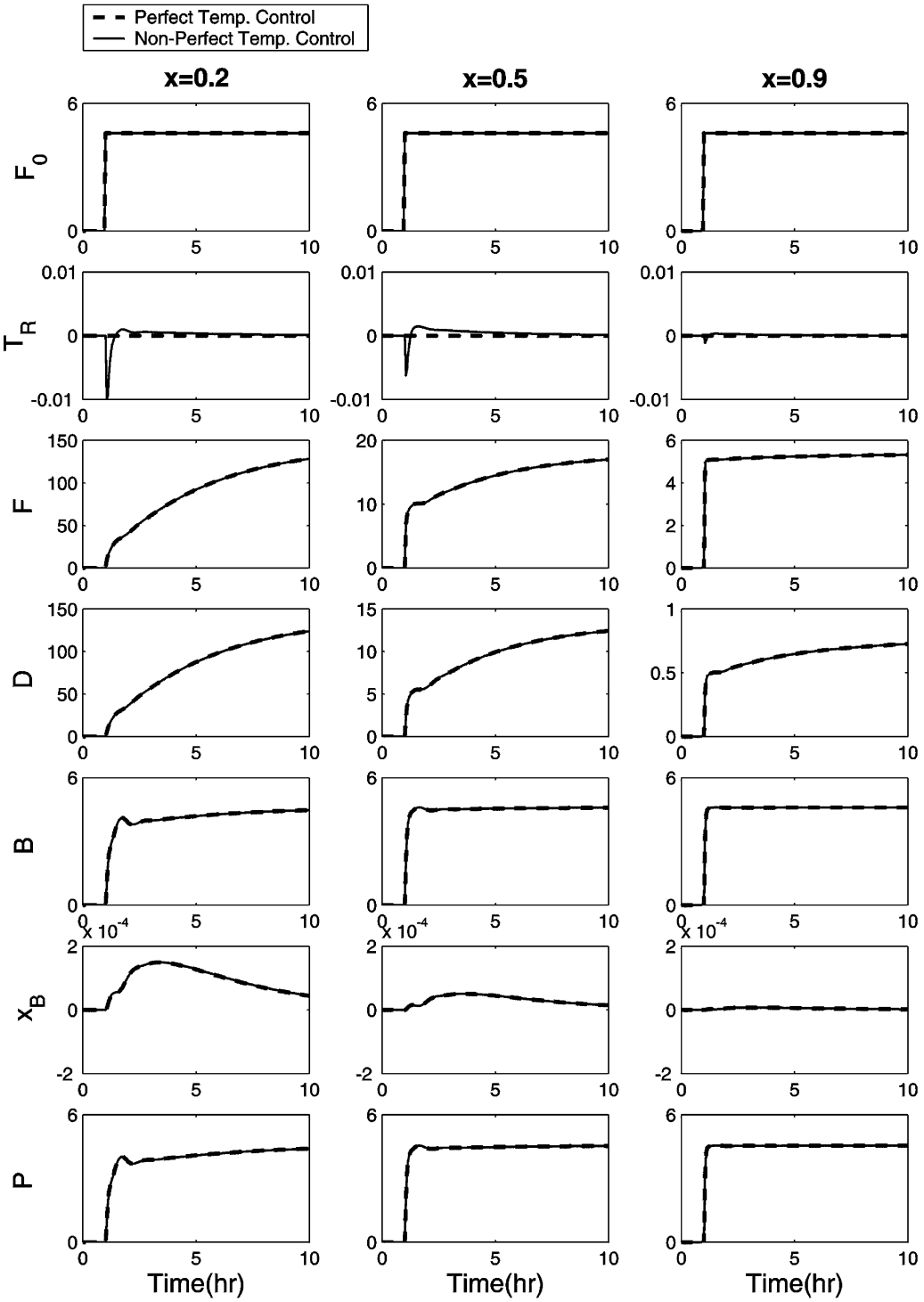

Figure 7. Reactor/separator dynamics for step change in feed flow with CS1 for different steady-state designs using a rigorous reactor/separator model assuming perfect reactor temperature control (dashed lines) and nonperfect reactor temperature control (solid lines).

place the poles such that the system has a closed-loop time constant as a fraction of the residence (i.e., $\tau_{CL} = \gamma\tau_R$) with a damping coefficient of $\zeta = 0.707$. This can be written as

$$G_L(s) = \frac{2\tau_{CL}\zeta s + 1}{{\tau_{CL}}^2 s^2 + 2\tau_{CL}\zeta s + 1} = \frac{2 \times 0.707(\gamma\tau_R)s + 1}{(\gamma\tau_R)^2 s^2 + 2 \times 0.707(\gamma\tau_R)s + 1} \quad (17)$$

After eq 7 is substituted for τ_R in eq 26, the controller parameters can be expressed as

$$K_C = \frac{\sqrt{2}}{\gamma}\frac{k(1-x)}{x} \quad (18)$$

$$\tau_I = \frac{\sqrt{2}x\gamma}{k(1-x)} \quad (19)$$

If we set $\gamma = 0.1$ (i.e., $\tau_{CL} = 0.1\tau_R$) and $\zeta = 0.707$, Figure 8 shows that the dynamic responses slow as the conversion increases (e.g., dashed lines in Figure 8 with $x = 0.5$ and 0.9). Figure 8 also reveals that perfect produc-

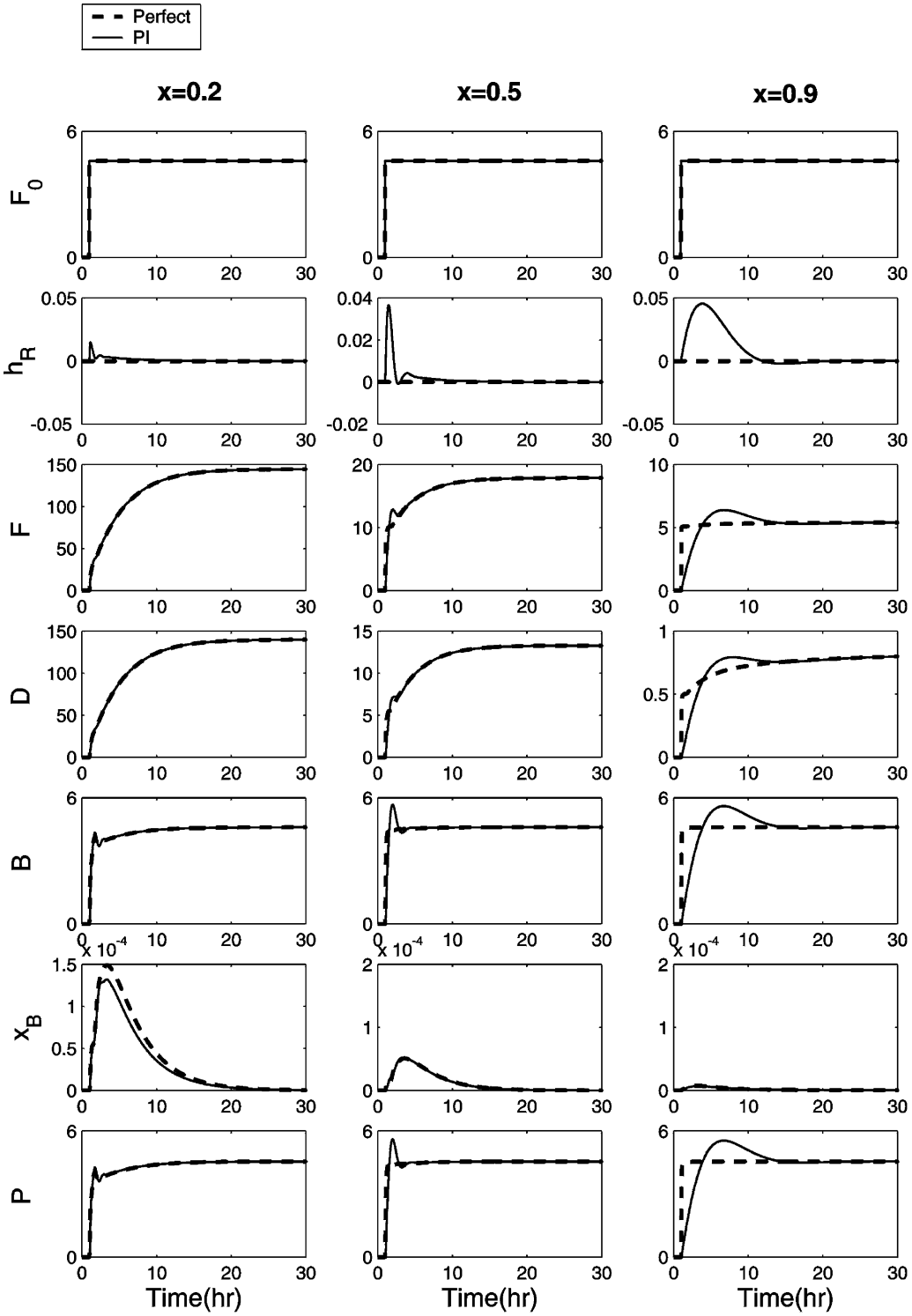

Figure 8. Reactor/separator dynamics for step change in feed flow with CS1 for different steady-state designs using a rigorous nonlinear model + perfect reactor level control (dashed lines) and a rigorous nonlinear model + conventional tuning for reactor level (solid lines).

tion rate changes can no longer be achieved, especially at high conversion.

With a PI reactor level control, the production rate dynamics in the recycle structure become

$$\frac{P(s)}{F_0(s)} = \frac{\left[\frac{2x\gamma}{\sqrt{2}k(1-x)}s + 1\right]\left(\frac{1}{k}s + 1\right)}{\frac{\gamma^2 x}{k^3(1-x)^2}s^3 + \left[\frac{\gamma^2}{k^2(1-x)^2} + \frac{2x\gamma}{\sqrt{2}k^2(1-x)}\right]s^2 + \left[\frac{2x\gamma}{\sqrt{2}k(1-x)} + \frac{1}{k}\right]s + 1} \quad (20)$$

This is a third-order system with the net order of 1. With the typical tuning constants, the root locus plot of the conversion (x varying from 0 to 1) is shown in Figure 9. It shows that, initially, the first pole (p_1) starts from the far left of the real axis and the other two poles are located at finite positions (p_2, $p_3 = k(-1 \pm \sqrt{1-4\gamma^2})/2\gamma^2$). The first two poles ($p_1$ and p_2) converge to the origin as the conversion increases, and the third pole (p_3) does not move much and was eventually canceled out by the zero ($z = -k$ in eq 20) as the conversion approaches 1 (i.e., $x \rightarrow 1$). The analysis

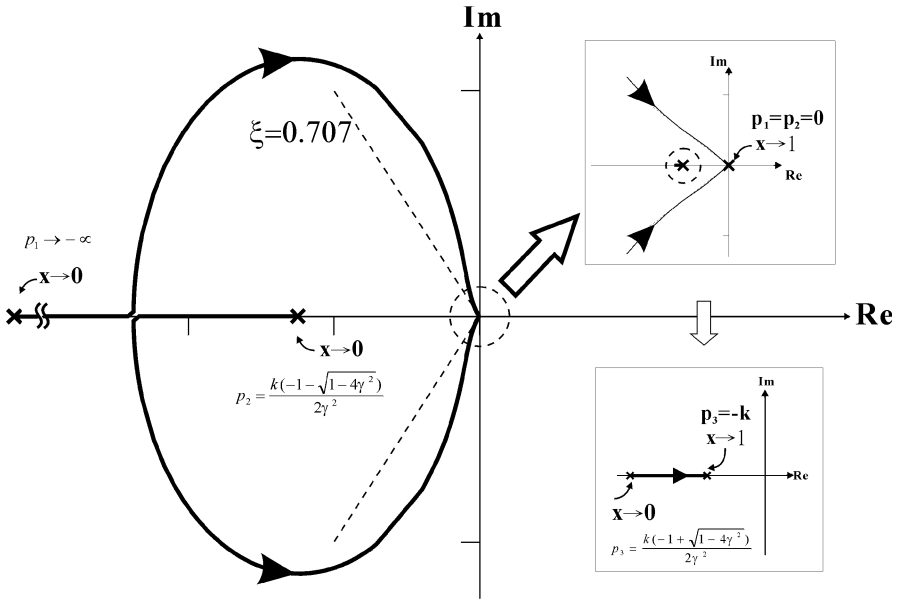

Figure 9. Root locus plot with varying reactor conversion (x changing from 0 to 1) for the reactor/separator process with CS1 and a typical reactor level control setting ($\gamma = 0.1$).

clearly indicates that, with a specification of $\gamma = 0.1$ and $\zeta = 0.707$ for the reactor level, the production dynamics becomes slower as the conversion increases and will eventually reach the origin as shown in Figure 9, and this explains the discrepancy between the perfect level control and PI level control. The difference becomes more evident at high conversion (e.g., $x = 0.9$ in Figure 8).

Equation 20 indicates that the closed-loop time constant ($\tau_{CL} = \gamma\tau_R$) is effective in adjusting the production dynamics. If γ is set to zero, we have a perfect reactor level control as well as perfect production control, i.e., $(P/F_0)(s) = 1$, and if we increase γ, the poles move toward the origin as shown in Figure 10. This was confirmed by nonlinear simulation of the recycle process, where Figure 11 clearly indicates that the production dynamics becomes slower when we slowly increase γ. For $x = 0.9$, the time constant of the total production (P) changes from 0 to 10 h as γ varies from 0 to 0.5 (Figure 11). Therefore, the reactor level control is crucial for the input/output dynamics of recycle processes and, for the case of high conversion, we can tighten the level loop tunings by specifying the dominant pole placement location for overall production dynamics (eq 20). To maintain a faster dynamic response, the closed-loop time constant to the residence time ratio (γ) has to be changed for different conversions. Here, we set the real part of the dominant pole at a specific location, as indicated by the vertical dashed line in Figure 10A, and this is equivalent to $\gamma = 0.01$ for the case of $x = 0.9$. Figure 12 compares the dynamics of perfect level control, using original tuning (i.e., typical tuning for the reactor level), and tightens the reactor level tuning. The results show that almost perfect production dynamics can be obtained by tightening the reactor level loop.

4. Extension to the Balanced Control Structure (CS2)

4.1. Linear Analysis. This class of control structures uses the reactor holdup to handle production rate variation,[17,28,29] and it is termed the balanced control structure. As shown by Wu et al.,[29] a simple implementation of the balanced control structure is to use a P-only controller for the reactor level, with the reactor effluent as the manipulated variable while the controller gain is set to $K_C = 1/\tau_R$. In doing this, the reactor holdup change is proportional to the flow variation. In other words, we are keeping a constant residence time ($\tau_R = V_R/F$). After substituting the overall material balance into eq 7 for the residence time, we have

$$\frac{F(s)}{F_{in}(s)} = \frac{1}{\tau_R s + 1} = \frac{1}{\frac{x}{k(1-x)}s + 1} \tag{21}$$

4.1.1. Reactor. The basic difference between these two structures lies in the reactor level control strategy. In the conventional structure, reactor holdup is fixed and, in the present case, the residence time ($\tau_R = V_R/F$) is kept constant. Following a similar approach, the component material balance equation (eq 2) can be linearized first, followed by taking Laplace transformation. Thus, one obtains

$$\frac{F_A(s)}{F_{in}(s)} = \frac{1-x}{\frac{x}{k}s + 1} \tag{22}$$

$$\frac{F_B(s)}{F_{in}(s)} = \frac{x}{\left(\frac{x}{k}s + 1\right)\left[\frac{x}{k(1-x)}s + 1\right]} \tag{23}$$

The results indicate that the systems have two poles. The first one, the same as the previous case, is located at $p_1 = -k/x$, and the second one is $p_2 = -k(1-x)/x$. Both poles start at the far left at low conversion and, at high conversion, the first pole (p_1) converges to $-k$ while the second pole (p_2) moves toward the imaginary axis. This implies that the reactor dynamics can be extremely slow at high conversion. The reason for this slowdown comes from the large reactor residence for high conversion.

4.1.2. Recycle Plant. If we separate the reactor level dynamics from the level dynamics, the transfer func-

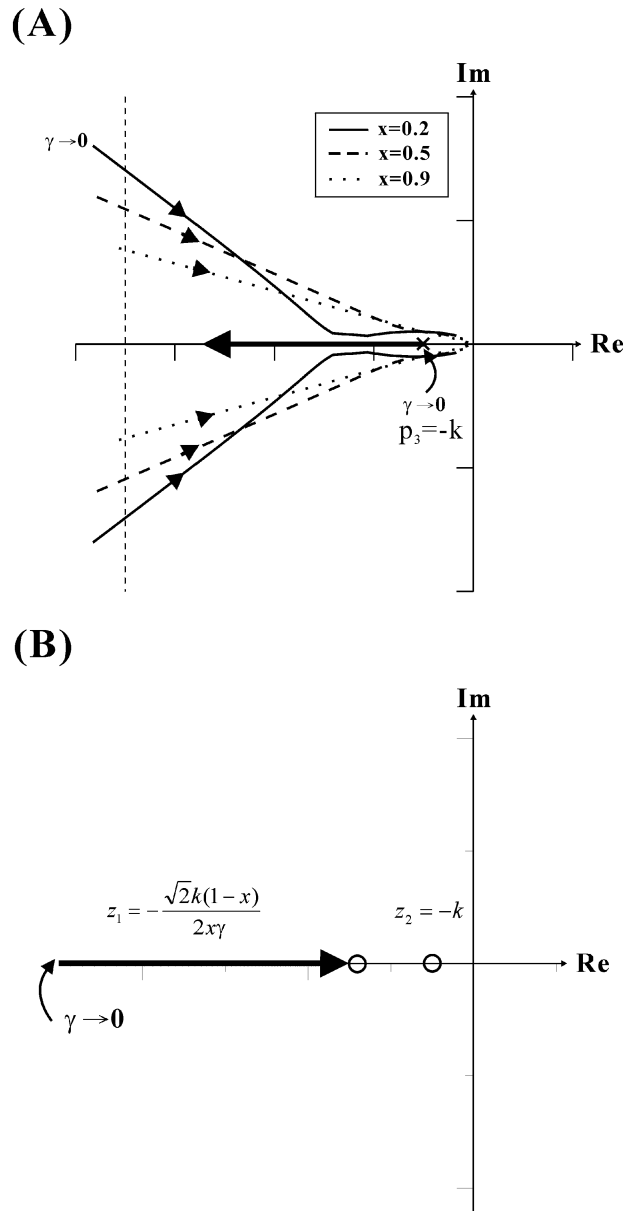

Figure 10. Root locus plot with varying reactor level setting (γ changing from 0 to 1) for different conversions (x = 0.2, 0.5, and 0.9): (A) all three pole configurations (the dashed vertical line indicating γ = 0.01, which is recommended for high conversion cases); (B) two zero configurations.

tions in the recycle block diagram (Figure 2) are

$$G_L = \frac{1}{\frac{x}{k(1-x)}s + 1} \tag{24}$$

$$G_R = \frac{(1-x)\left[\frac{x}{k(1-x)}s + 1\right]}{\frac{x}{k}s + 1} \tag{25}$$

$$G_P = \frac{x}{\frac{x}{k}s + 1} \tag{26}$$

Substituting these transfer functions into the positive feedback structure, we have the following recycle dynamics. Note that this is obtained by assuming perfect separation with no recycle dynamics.

$$\frac{P(s)}{F_0(s)} = \frac{1}{\left(\frac{1}{k}s + 1\right)\left[\frac{x}{k(1-x)}s + 1\right]} \tag{27}$$

$$\frac{D(s)}{F_0(s)} = \frac{1-x}{x}\cdot\frac{1}{\frac{1}{k}s + 1} \tag{28}$$

$$\frac{F(s)}{F_0(s)} = \frac{1}{k}\frac{\left(\frac{x}{k}s + 1\right)}{\left(\frac{1}{k}s + 1\right)\left[\frac{x}{k(1-x)}s + 1\right]} \tag{29}$$

Some observations can be made immediately.

1. As the conversion increases, one of the poles (p_2 in Figure 5A) of the product flow dynamics moves from the far left toward the origin. Equation 27 clearly shows that the *input/output* dynamics become slower as the conversion increases.

2. For different conversions (x) in design, the pole of *recycle* flow dynamics [$D(s)/F_0(s)$] is invariant and it is located at $p = -k$ as shown in Figure 5B.

3. As the conversion (x) increases, one of the poles (p_2) of *reactor effluent* dynamics [$F(s)/F_0(s)$] moves toward the origin while the zero converges to $z = -k$ (Figure 5C).

4. The steady-state sensitivity of the recycle flow (D) to the fresh feed flow (F_0) varies from infinity to 0 as the conversion (x) changes from 0 to 1, as indicated in eq 28. In terms of absolute flow rates, the ratio is $D/F_0 = (1-x)/x$ and, expressed in percent deviation, the ratio becomes $(D/\bar{D})/(F_0/\bar{F}_0) = 1$.

Obviously, for a recycle structure (Figure 2), the level control strategies lead to totally different recycle dynamics. Perfect production control is no longer achievable under the case of variable reactor holdup. At small conversion, the recycle dynamics is comparable to that of the case of fixed reactor holdup. As the conversion increases (i.e., a larger reactor), the residence time increases and slower dynamics results (eq 16), as shown in Figure 13. However, the sensitivity of the recycle flow to the production rate variation, the snowball effect, is alleviated as indicated in observation 4. Actually, the percent change in the recycle flow is exactly the same as that of the feed flow, and this is exactly the objective of the balanced control structure, handling production rate changes using the reactor holdup.

4.1.3. Dynamic Responses. Again, three design alternatives for the simple recycle process are studied, and they belong to low conversion (x = 0.2), moderate conversion (x = 0.5), and high conversion (x = 0.9). The dashed lines in Figure 14 indicate that slower production dynamics is observed at high conversion (e.g., x = 0.9 in Figure 14). The recycle flow dynamics is about the same for all three conversions, while the reactor effluent dynamics follows a similar pattern as that of production dynamics. As for the recycle flow sensitivity, the recycle flows increase 10% (x = 0.2, 0.5, and 0.9) for a 10% step increase in the production rate.

4.2. Validation. 4.2.1. Nonlinear Reactor. Because the production rate variation is handled by changing the reactor holdup, the reactor level dynamics has a time constant of τ_R with a proportional gain of $K_C = 1/\tau_R$. Again, a nonlinear isothermal CSTR is assumed while using a perfect separator. For a 1% step increase in the

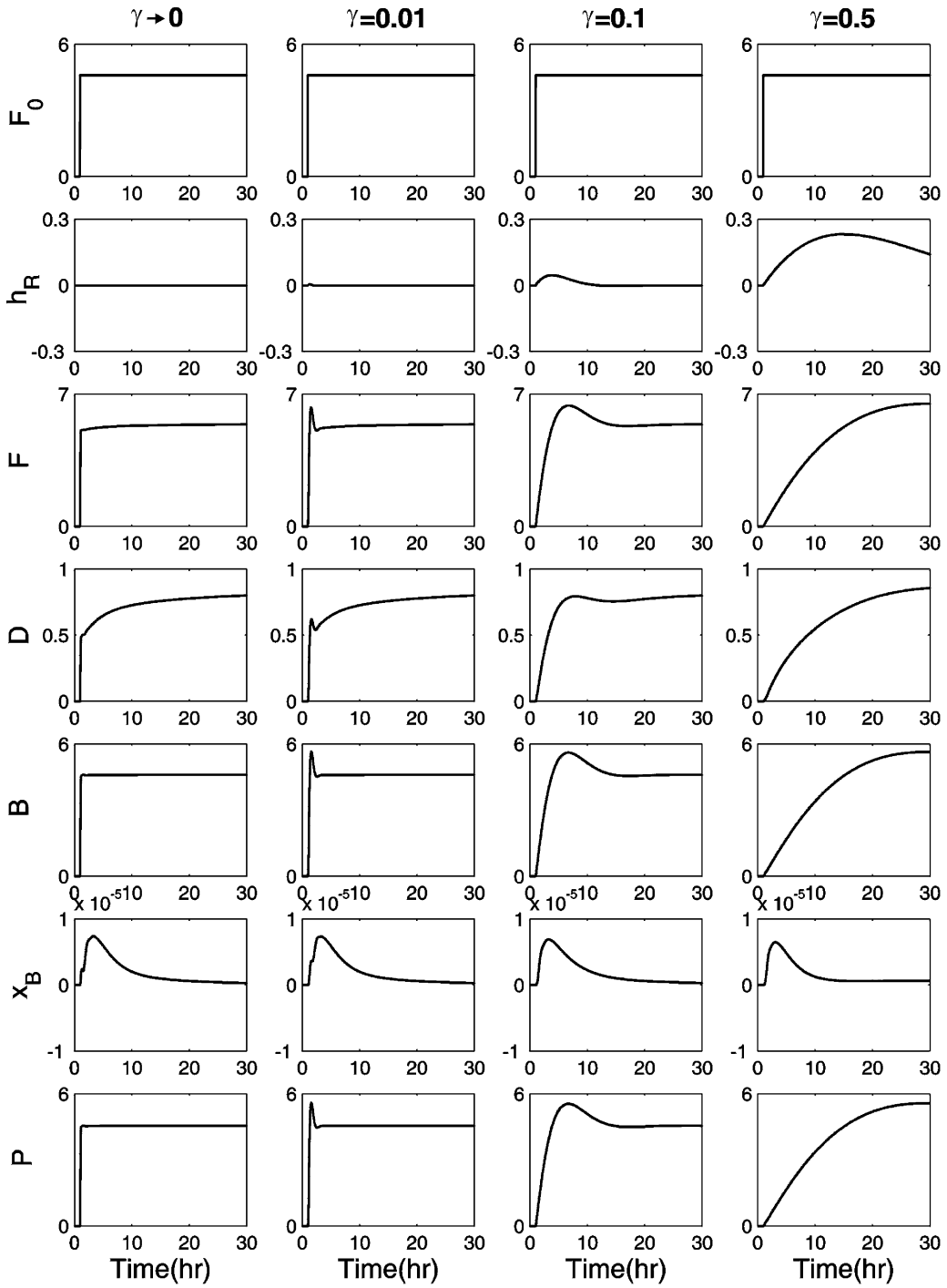

Figure 11. Rigorous reactor/separator dynamics for step change in feed flow with CS1 and $x = 0.9$ using different degrees of tightness in the level loop ($\gamma \rightarrow 0 \Rightarrow$ perfect level control).

fresh feed flow, we have almost the same responses as those of a linearized model (solid lines in Figure 14). Again, a very good approximation can be obtained using the linearized model. Notice that as the step size increases (e.g., 5%), visible deviations in the recycle flows can be observed for the low conversion case (e.g., $x = 0.2$) while the high conversion case still shows a reasonably good behavior description.

4.2.2. Rigorous Distillation. Similar to the case of constant reactor holdup, a nonlinear distillation column is employed. This has exactly the balanced control structure of the recycle process studied in refs 4 and 29. Again, three alternative designs (low, moderate, and high conversions) are studied, and parameter values are given in Table 1. The process flowsheet is exactly the same as Figure 5, but a P-only reactor level control is employed with $K_C = 1/\tau_R$. The composition controller is also set with the modified Ziegler−Nichols tuning.[25]

Simulation results clearly show that the production dynamics, P in Figure 15, become slower as the conversion increases. Figure 15 also reveals that much better composition control, x_B, can be achieved as compared to that of the constant reactor holdup (x_B in Figure 6), especially at low conversion, but with this dynamics, the total production is much slower compared to the case of constant reactor holdup (P in Figure 6). Results also reveal that the linear recycle models provide a very good description of the true process.

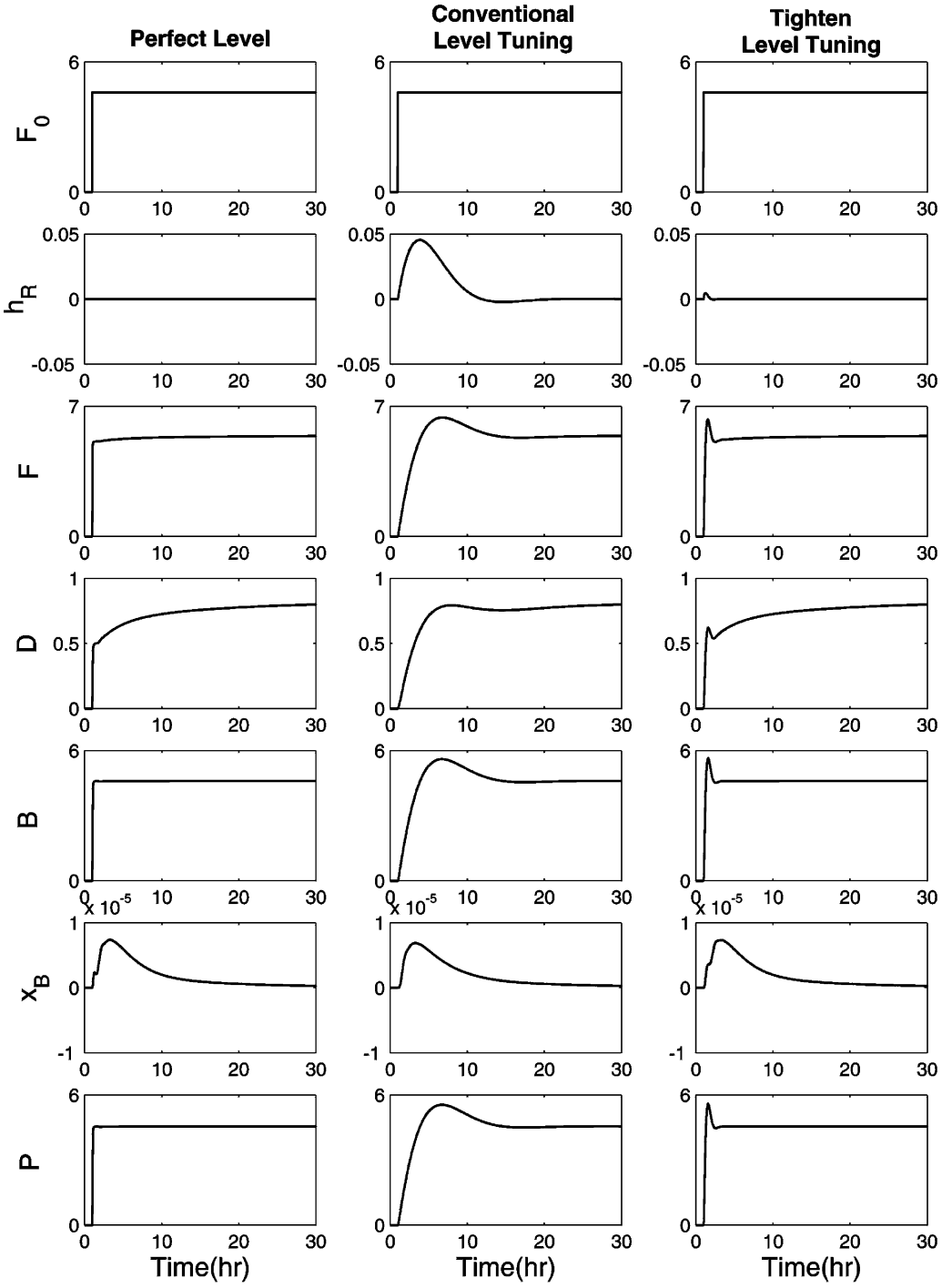

Figure 12. Rigorous reactor/separator dynamics for step change in feed flow with CS1 and $x = 0.9$ using perfect level control, conventional reactor level tuning (keeping a fixed open-loop/closed-loop time constant ratio), and tightened reactor level tuning.

5. Implications for Control

5.1. Tradeoffs between Steady-State Sensitivity and Dynamic Responsiveness. Rigorous nonlinear simulations confirm that the linear analysis (Figure 2) provides good behavior description for the recycle process and the observations in section 2 are generally valid for the material recycle process. These two control structures, CS1 and CS2 in Figure 5, possess different characteristics. In terms of dynamic responsiveness, near-perfect production rate variations can be achieved over the entire range of conversion for CS1 (e.g., Figure 12) and, for CS2, variable reactor holdup, sluggish production dynamics is observed at high conversion (e.g., Figure 15). As for steady-state sensitivity, a severe snowball effect is observed for the control structure with constant V_R and the sensitivity reaches infinity when the conversion approaches zero (e.g., observation 4 in section 2.1.2). This imposes an inherent limitation on the operability for CS1. For example, if the maximum flow rate of each stream is twice its nominal value (e.g., $F_{max} = 2\bar{F}$), it can be shown that the maximum percentage of the production rate increase can be simply given by

$$\Delta(P/\bar{P})_{max} = 100\frac{x}{1+x} \tag{30}$$

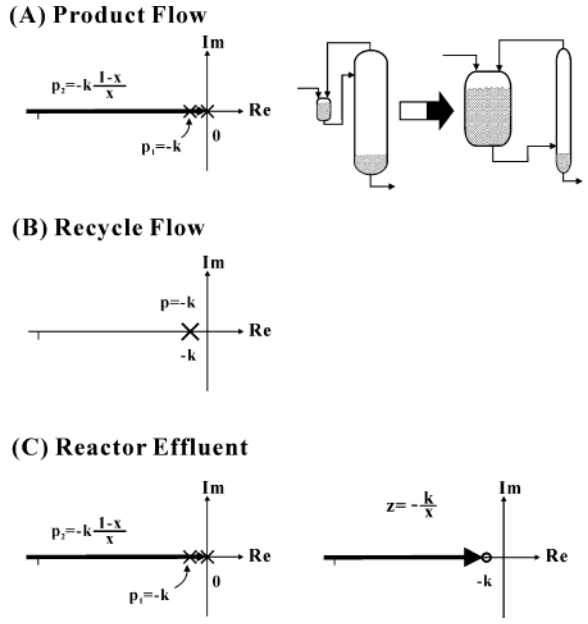

Figure 13. Root locus with varying conversion for the reactor/separator process with CS2 for (A) product flow dynamics (× indicating converging pole and fixed pole locations), (B) recycle flow dynamics (× indicating a fixed pole), and (C) reactor flow dynamics (× indicating converging pole and fixed pole locations and ○ denoting converging zero location).

where x is the conversion. On the other hand, the operability for the CS2 control structure is much better and remains the same over the entire conversion. That is

$$\Delta(P/\bar{P})_{\max} = 100 \tag{31}$$

It should be emphasized that CS2 has a constraint involving the maximum reactor volume that potentially limits its operability, unless the reactor is operated at 50% of its capacity. Figure 16 indicates the production rate handling capabilities of these two control structures.

5.2. Control Structures at Different Conversions. Ongoing analyses clearly indicate that no single control structure works well over the entire range of conversion. The variable reactor holdup (CS2) is preferred at low conversion for its steady-state operability and not too slow dynamic responsiveness, and at moderate to high conversion, the constant V_R (CS1) is a better choice for its dynamic responsiveness and acceptable steady-state operability. The boundary is determined by the turndown ratio of design. For example, if the maximum production rate is set to at least 125% of its nominal value (i.e., $P_{\max} = 1.25\bar{P}$), from eq 30, we have $x = 0.25/(1 - 0.25) = {}^1/_3$. This implies that, if $x < {}^1/_3$, the variable reactor holdup structure (CS2) is preferred and the constant V_R (CS1) should be used for $x \geq {}^1/_3$. The thick solid lines in Figure 16 show the corresponding control structure at different conversions.

5.3. Ideal Control Structure. Can we devise a control structure such that the tradeoff between steady-state operability and dynamic responsiveness can be avoided? Before answering this question, it should be

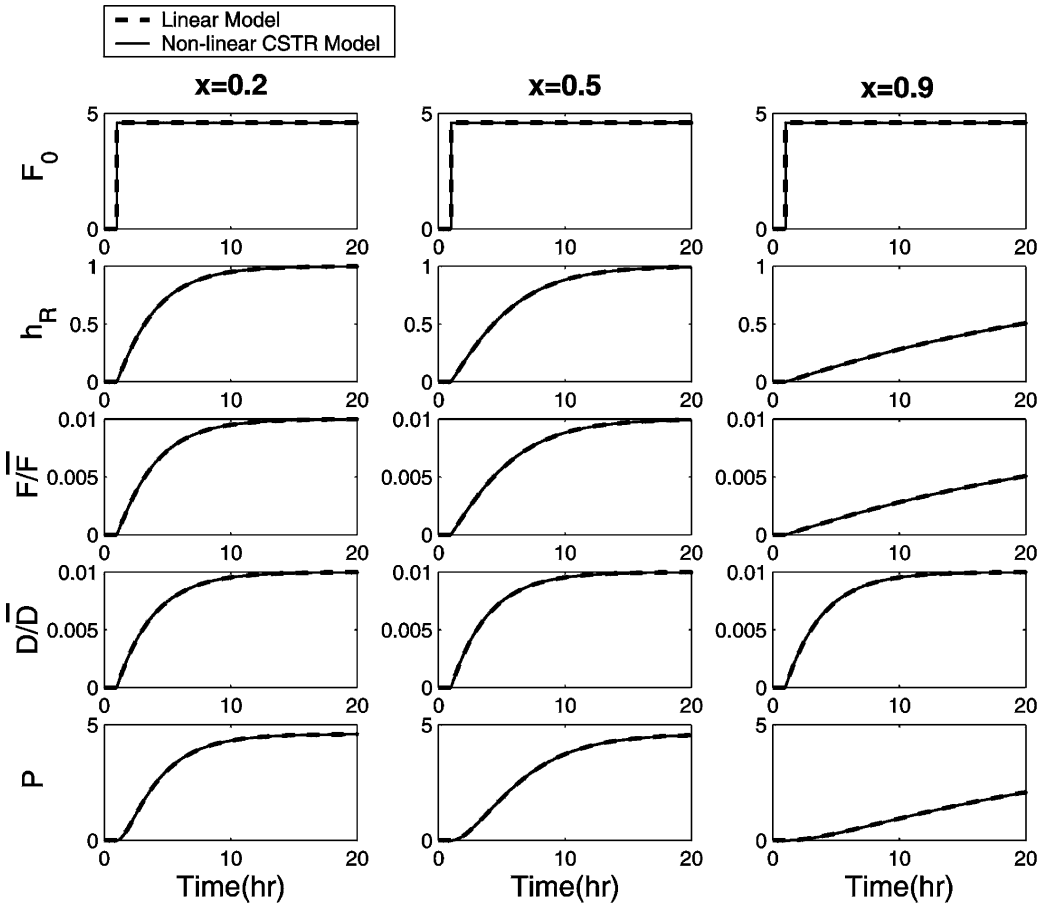

Figure 14. Reactor/separator dynamics for step change in feed flow with CS2 for different steady-state designs using a linear model (dashed lines) and a nonlinear CSTR model + perfect separator (solid lines).

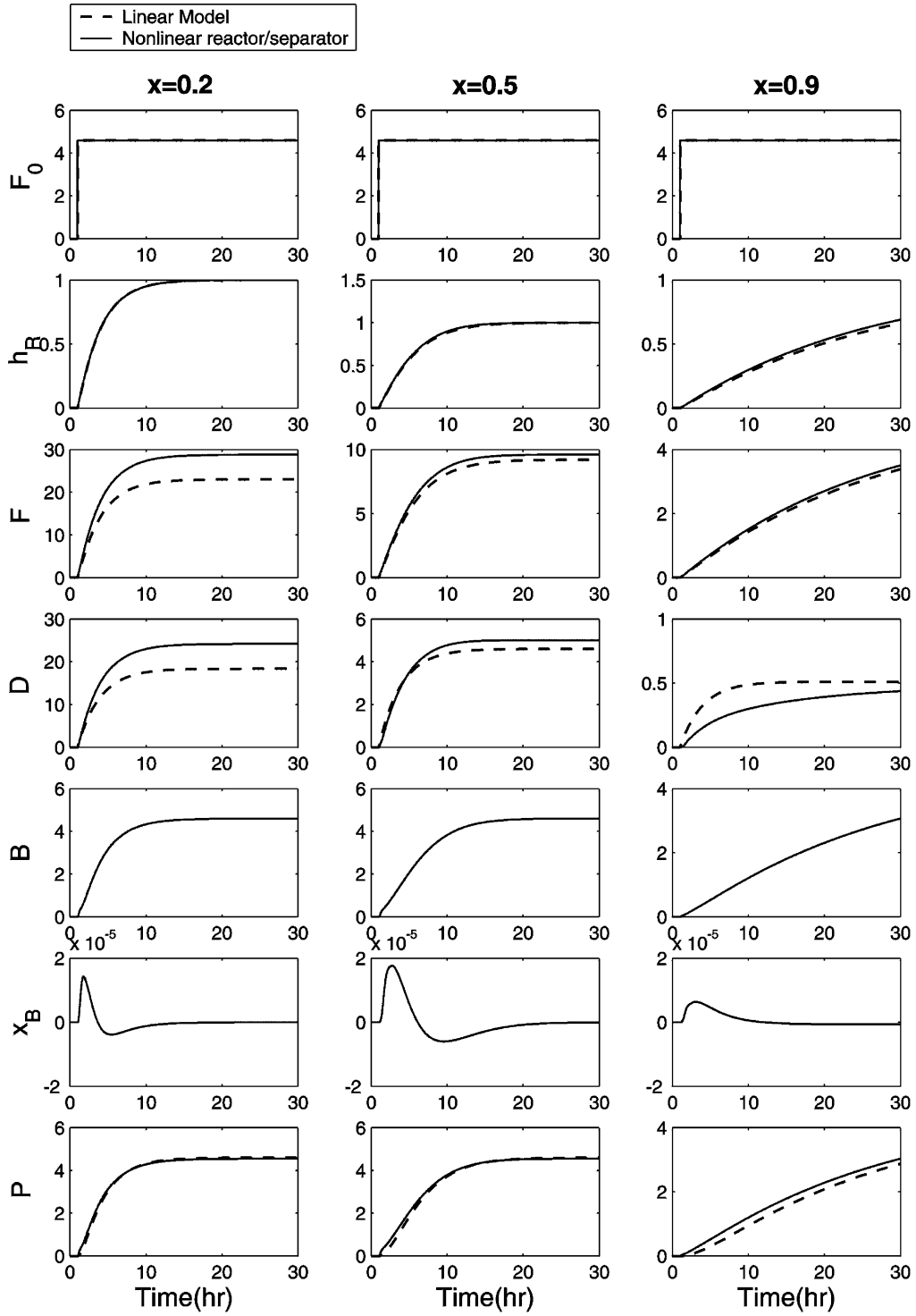

Figure 15. Reactor/separator dynamics for step change in feed flow with CS2 for different steady-state designs using a linear model (dashed lines) and a rigorous reactor/separator model + P reactor level control (solid lines).

understood that the sluggishness in the production rate change originated from the reactor level dynamics and, for CS2, such a sluggish tuning comes from a change in the reactor holdup in proportion to the flow rate. Therefore, if we can handle the production rate variation using some variable without affecting flow dynamics, the tradeoffs can be eliminated. The reactor temperature is one obvious choice, as shown in eq 1. This is exactly the third control structure (CS3) mentioned in section 2. Figure 17 shows that, in CS3, the production rate is set by the fresh feed flow and the reactor temperature is adjusted according to the fresh feed flow via a feedforward controller. Similar to CS1, tight controller settings are required for the reactor level.

With the reactor temperature as the throughput manipulator (CS3), near-perfect production can be achieved while maintaining good steady-state operability as shown in Figure 18, as compared to CS1. Certainly, CS3 is only applicable to the situation where a wide range of reactor temperature variation can be practiced.

Before leaving the section, one control strategy not addressed in the paper involves on-demand production rate. Here the base stream from the column is flow-

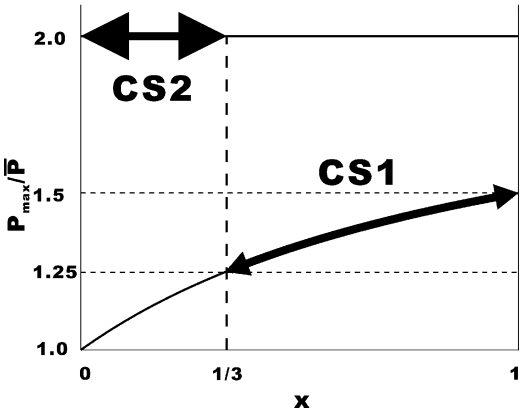

Figure 16. Recommended control structure using the maximum achievable production rate ($P_{max} = 1.25\bar{P}$) as a criterion: CS1 and CS2.

controlled, with the setpoint coming from the downstream unit that demands instantaneous rate changes. In this case what part of the analysis in this paper applies to this situation? The step input in the fresh feed results in a step output in the total production (considering CS1 with perfect reactor level control). This implies that, for the on-demand structure, perfect control can also be achieved if the fresh feed also shows a steplike input. This can be achieved by the proper design of the level controller (assuming using base level to control the column feed). That is the column base level controller should be able to give the following relationship:

$$\frac{F(s)}{P(s)} = \frac{G_L}{1 - G_L G_R} = \frac{\frac{1}{kx}s + \frac{1}{x^2}}{\frac{1}{k}s + 1}$$

If one chooses to use a ratio scheme [$(D + F_0)/P$], the ratio controller should have the following dynamics:

$$\frac{D + F_0(s)}{P(s)} = \frac{\frac{1 - x}{kx}s + \frac{1 - x^2}{x^2}}{\frac{1}{k}s + 1} + 1$$

These two relationships come directly from eqs 14 and 15. In summary, the results can be extended to the on-demand control structure under different control configurations.

6. Conclusion

This work shows that linear transfer-function-based analysis facilitates the evaluation of process dynamics at the design stage and, more importantly, input/output dynamics depends on the control structure. Therefore, a preliminary decision on the control structure, i.e., determining the throughput manipulator, has to be made to assess the dynamic performance at the design stage.

In this work a simple recycle process with a first-order irreversible reaction is studied. In the modeling phase, the total flows of different components (F_A and F_B) are parametrized as state variables, instead of using the typical composition (z_A and z_B). For the case of constant reactor holdup (CS1), as opposed to one's intuition, linear analysis indicates that perfect production rate changes can *always* be achieved over the *entire range of conversion*. The reason is that the effects of the reactor dynamics and recycle gain compensate for each other, and perfect production is, thus, obtained for *input/output* dynamics while the *internal* dynamics is characterized as the rate constants (k). However, extreme steady-state sensitivity (also known as the snowball effect) is observed at low conversion. Linear analysis is validated using rigorous nonlinear simulations via a step-by-step relaxation on assumptions. The results also reveal the important role the reactor level dynamics play in dynamic responsiveness. and near-perfect input/output dynamics can be obtained by tightening the reactor level settings.

This approach is extended to the balanced control structure (CS2), and results show that input/output

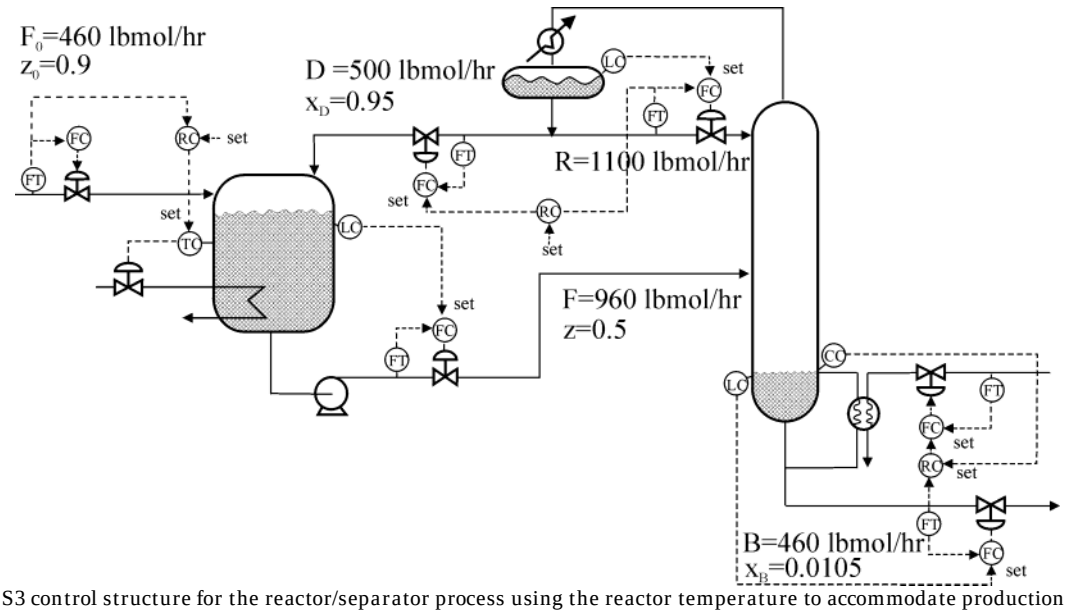

Figure 17. CS3 control structure for the reactor/separator process using the reactor temperature to accommodate production rate variation.

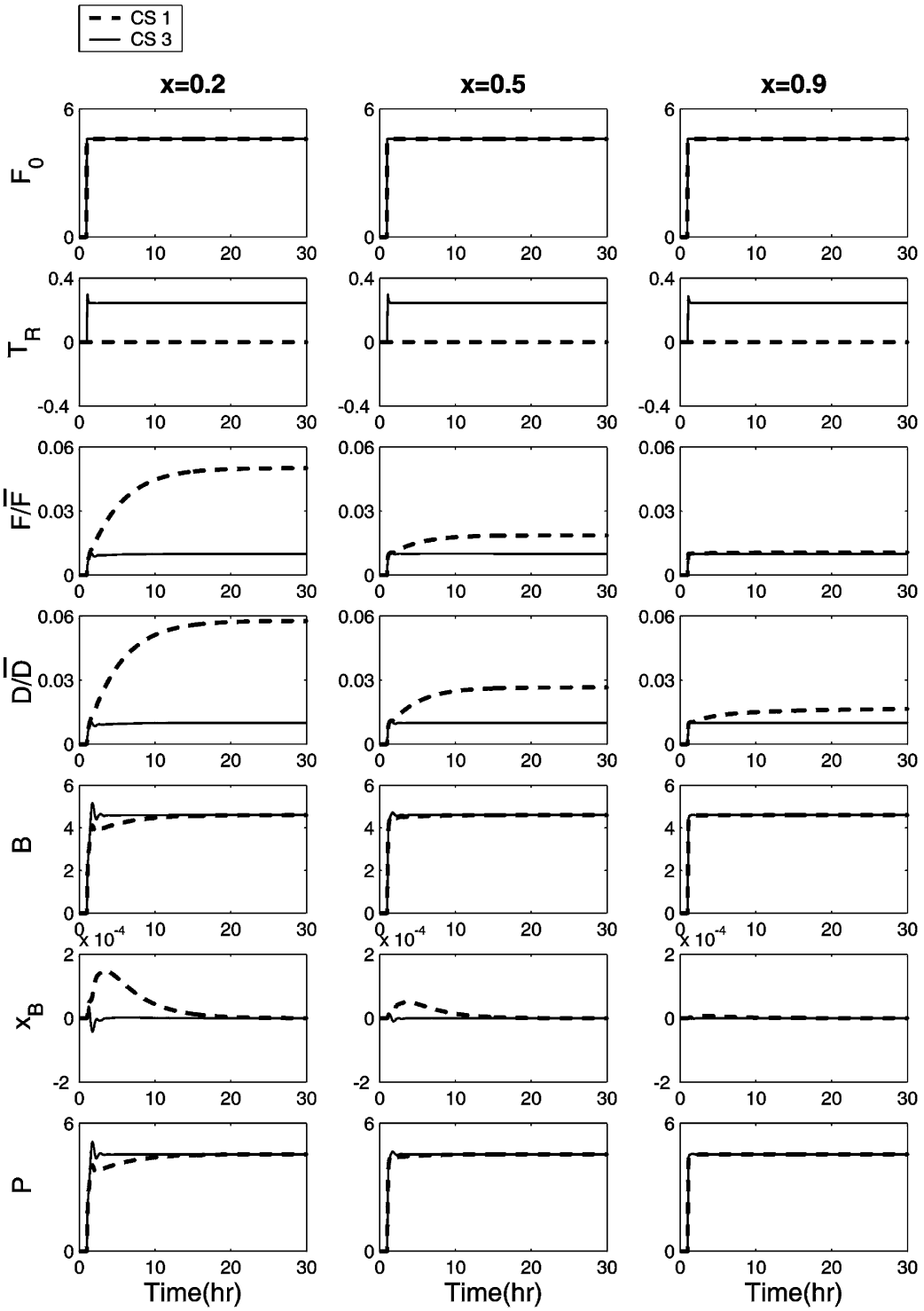

Figure 18. Reactor/separator dynamics for step change in feed flow for different steady-state designs using different control structures: CS1 (dashed lines); CS3 (solid lines).

dynamics varies with conversion. In particular, when the convergence approaches unity (i.e., $x \rightarrow 1$), an almost integrator response is observed. However, the steady-state sensitivity is invariant [i.e., $(D/\bar{D})/(F_0/\bar{F}_0) = 1$] over the entire range of conversion.

The proposed linear analysis clearly reveals tradeoffs between steady-state sensitivity and dynamic responsiveness. It is further extended to devise an ideal control structure (CS3) to achieve dynamic responsiveness while maintaining steady-state operability.

Acknowledgment

Financial support of the National Science Council of Taiwan is gratefully acknowledged. FORTRAN code for the nonlinear recycle plant is available upon request.

Appendix: Temperature Effect on Controllability for a Reactor in a Recycle Plant

Luyben[15] uses the temperature difference between the reactor (T_R) and the jacket (T_J) as a measure of the robustness and flexibility of the reactor system (i.e., ΔT

$= T_R - T_J$). The controllability is inversely proportional to the temperature difference (ΔT). The reason for using ΔT as a measure can be seen from the energy balance equation. Assume that the reactant is heated to the reaction temperature

$$(kV_R z_A)\lambda = UA\Delta T \tag{A1}$$

where λ is the exothermic heat of reaction and assumed to be a positive value, U is the overall heat-transfer coefficient, and A is the jacketed area. Typically, the reactor stability is limited by the heat removal capability, especially a limited heat-transfer area (A). A small ΔT implies that we have an excessive heat-transfer area, and only a small temperature difference is required to remove the heat generated from the reaction. On the other hand, if A is too small, then a large ΔT will be needed to remove the heat. Also note that the heat-transfer area (A) is not an independent variable and it is a function of the reactor volume. Letting the aspect ratio of the reactor be n (i.e, n = reactor height/reactor diameter), the relationship between the jacket area (A) and reactor holdup V_R (or volume) then becomes

$$A = (16n\pi)^{1/3} v^{2/3} {V_R}^{2/3} \tag{A2}$$

where v is the molar volume (because the reactor holdup is in lb mol). Assuming a pure reactant and from eq A1, the controllability measure becomes

$$\Delta T = \frac{kV_R(1-x)\lambda}{U(16n\pi)^{1/3} v^{2/3} {V_R}^{2/3}} = \frac{k\lambda}{U(16n\pi)^{1/3} v^{2/3}}(1-x){V_R}^{1/3} \tag{A3}$$

For a given fresh feed flow (F_0), from eq 7 and the relationship between the conversion (x) and the reactor feed flow (F), V_R can be expressed as

$$V_R = \frac{Fx}{k(1-x)} = \frac{F_0}{k(1-x)} \tag{A4}$$

Substituting eq B4 into eq B3, one obtains

$$\Delta T = \frac{k\lambda}{U(16n\pi)^{1/3} v^{2/3}}(1-x)\left[\frac{F_0}{k(1-x)}\right]^{1/3} = \frac{\lambda {F_0}^{1/3} k^{2/3}}{U(16n\pi)^{1/3} v^{2/3}}(1-x)^{2/3} \tag{A5}$$

Equation A5 is useful in evaluating reactor controllability for many possible scenarios. For a given production rate and reaction kinetics, the only design variable is the conversion (x), and eq A5 clearly indicates that a larger conversion implies a smaller ΔT and, thus, better controllability. This gives exactly the opposite results compared to the case of scaling up of a reactor.[6]

Nomenclature

A = reactor jacket area
A = reactant
B = product
B = product flow rate (from the bottom of the distillation)
CS1 = control structure with constant reactor holdup (using z_A to handle the production rate variation)
CS2 = control structure with variable reactor holdup (using V_R to handle the production rate variation)
CS3 = control structure with variable reactor temperature (using T to handle the production rate variation)
$D(s)$ = recycle flow rate (distillate flow in the distillation column)
$\bar{D}$ = nominal value of the recycle flow rate (distillate flow in the distillation column)
E = activation energy
$F(s)$ = reactor effluent flow rate (mol/h)
$\bar{F}$ = nominal value of the reactor effluent flow rate
F_A = total flow rate of reactant A ($F_A = Fz_A$) (mol/h)
F_B = total flow rate of product B ($F_B = Fz_B$) (mol/h)
$F_{in}(s)$ = reactor inlet flow rate (mol/h)
$\bar{F}_{in}$ = nominal value of the reactor inlet flow rate (mol/h)
$F_0(s)$ = fresh feed flow rate (mol/h)
$\bar{F}_0$ = nominal value of the fresh feed flow rate (mol/h)
$G_L(s)$ = reactor level dynamics
$G_R(s)$ = reaction and separation dynamics for reactant A
$G_P(s)$ = reaction and separation dynamics for product B
k = reaction rate constant
k_0 = preexponential factor for the rate constant
K_C = controller gain
n = aspect ratio of a reactor (height/diameter)
p_i = ith pole of a transfer function
$P(s)$ = total production rate [i.e., $P = (1 - x_B)B = F_B$] (mol/h)
$\bar{P}$ = nominal value of the production rate (mol/h)
$R(s)$ = reflux flow rate in the distillation column (mol/h)
$\bar{R}$ = nominal value of the reflux flow rate in the distillation column (mol/h)
T_J = reactor jacket temperature
T_R = reactor temperature
U = overall heat-transfer coefficient
v = molar volume
V_R = reactor holdup (mol)
x = conversion in the reactor
x_B = bottom product composition (mole fraction)
x_D = distillate composition (mole fraction)
z_A = reactor composition of A (mole fraction)
z_B = reactor composition of B (mole fraction)
z_i = ith zero of the transfer function

Greek Symbols

ΔT = difference between the reactor temperature and the jacket temperature (used as a controllability measure)
λ = exothermic heat of reaction (a positive value)
γ = fraction of the residence time
τ_{CL} = closed-loop time constant ($\tau_{CL} = \gamma\tau_R$)
τ_I = reset time
τ_R = residence time for the reactor
ζ = damping coefficient

Literature Cited

(1) Bildea, C. S.; Dimian, A. C.; Iedema, P. D. Nonlinear Behavior of Reactor−Separator−Recycle Systems. *Comput. Chem. Eng.* **2000**, *23*, 209.

(2) Chen, Y. H.; Yu, C. C. Interaction between Thermodynamic Efficiency and Dynamic Controllability: Heat-Integrated Reactor. *Comput. Chem. Eng.* **2000**, *23*, 1077.

(3) Chen, Y. H.; Yu, C. C. Dynamical Properties of Product Life Cycle: Implications to the Design and Operation of Industrial Processes. *Ind. Eng. Chem. Res.* **2001**, *40*, 2452.

(4) Cheng, Y. C.; Wu, K. L.; Yu, C. C. Arrangement of Throughput/Inventory Control in Plantwide Control. *J. Chin. Inst. Chem. Eng.* **2002**, *33*, 283.

(5) Denn, M. M.; Lavie, R. Dynamics of Plants with Recycle. *Chem. Eng. J.* **1982**, *24*, 55.

(6) Devia, N.; Luyben, W. L. Reactors: Size versus Stability. *Hydrocarbon Process.* **1978**, *57* (6), 119.

(7) Gilliland, E. R.; Gould, L. A.; Boyle, T. J. Dynamic Effects of Material Recycle. Proceedings of the Joint Automatic Control Conference, Stanford University, 1964; p 140.

(8) Jacobsen, E. W. On the Dynamics of Integrated Plants—Non-Minimum Phase Behavior. *J. Process Control* **1999**, *9*, 439.

(9) Kapoor, N.; McAvoy, T. J.; Marlin, T. E. Effect of Recycle Structure on Distillation Tower Time Constants. *AIChE J.* **1986**, *32*, 411.

(10) Kiss, A. A.; Bildea, C. S.; Dimian, A. C.; Iedema, P. D. State Multiplicity in CSTR−Separator−Recycle Polymerisation Systems. *Chem. Eng. Sci.* **2002**, *57*, 535.

(11) Kwok, K. E.; Chong-Ping, M.; Dumont, G. A. Seasonal Model Based Control of Processes with Recycle Dynamics. *Ind. Eng. Chem. Res.* **2001**, *40*, 1633.

(12) Lakshminarayanan, S.; Takada, H. Empirical Modelling of Processes with Recycle: Some Insights via Case Studies. *Chem. Eng. Sci.* **2001**, *56*, 3327.

(13) Luyben, W. L. *Process Modeling, Simulation, and Control for Chemical Engineers*, 2nd ed.; McGraw-Hill: New York 1989.

(14) Luyben, W. L. Dynamics and Control of Recycle Systems. 1. Simple Open-Loop and Closed-Loop Systems. *Ind. Eng. Chem. Res.* **1993**, *32*, 466.

(15) Luyben, W. L. Dynamics and Control of Recycle Systems. 2. Comparison of Alternative Process Designs. *Ind. Eng. Chem. Res.* **1993**, *32*, 476.

(16) Luyben, W. L. Trade-offs between Design and Control in Chemical Reactor Systems. *J. Process Control* **1993**, *3*, 17.

(17) Luyben, W. L. Snowball Effect in Reactor/Separator Process with Recycle. *Ind. Eng. Chem. Res.* **1994**, *33*, 299.

(18) Luyben, W. L. Temperature Control of Autorefrigerated Reactors. *J. Process Control* **1999**, *9*, 301.

(19) Morud, J.; Skogestad, S. Dynamic Behavior of Integrated Plants. *J. Process Control* **1996**, *6*, 145.

(20) Ogunnaike, B. A.; Ray, W. H. *Process Dynamics, Modeling and Control*; Oxford University Press: Oxford, U.K., 1994.

(21) Papadourakis, A.; Doherty, M. F.; Douglas, J. M. Relative Gain Array for Units in Plants with Recycle. *Ind. Eng. Chem. Res.* **1987**, *26*, 1259.

(22) Pushpavanam, S.; Kienle, A. Nonlinear Behavior of an Ideal Reactor Separator Network with Mass Recycle. *Chem. Eng. Sci.* **2001**, *56*, 2873.

(23) Scali, C.; Ferrari, F. Performance of Control Systems Based on Recycle Compensators in Integrated Plants. *J. Process Control* **1999**, *9*, 425.

(24) Seborg, D. E.; Edgar, T. F.; Mellichamp, D. A. *Process Dynamics and Control*; Wiley: New York, 1989.

(25) Shen, S. H.; Yu, C. C. Use of Relay-Feedback Test for Automatic Tuning of Multivariable Systems. *AIChE J.* **1994**, *40*, 627.

(26) Taiwo, O. The Design of Robust Control Systems for Plants with Recycle. *Int. J. Control* **1993**, *43*, 671.

(27) Verykios, X. E.; Luyben, W. L. Steady-State Sensitivity and Dynamics of a Reactor/Distillation Column Systems with Recycle. *ISA Trans.* **1978**, *17* (2), 31.

(28) Wu, K. L.; Yu, C. C. Reactor/Separator Processes with Recycle—1. Candidate Control Structure for Operability. *Comput. Chem. Eng.* **1996**, *20*, 1291.

(29) Wu, K. L.; Yu, C. C.; Luyben, W. L.; Skogestad, S. Reactor/Separator Processes with Recycle—2. Design for Composition Control. *Comput. Chem. Eng.* **2003**, *27*, 421.

Received for review October 10, 2002
Revised manuscript received June 9, 2003
Accepted July 11, 2003

IE020799I